Journal of Power Sources 259 (2014) 166–176

Contents lists available at ScienceDirect

Journal of Power Sources

journal homepage: www.elsevier.com/locate/jpowsour

# Estimation of state-of-charge and state-of-power capability of lithium-ion battery considering varying health conditions

Fengchun Sun, Rui Xiong*, Hongwen He

*National Engineering Laboratory for Electric Vehicles, School of Mechanical Engineering, Beijing Institute of Technology, No. 5 South Zhongguancun Street, Haidian District, Beijing 100081, China*

## HIGHLIGHTS

- Robustness of the SoC estimator against varying health conditions is analyzed.
- Robustness of the SoP estimator against varying health conditions is analyzed.
- The need of parameter updates of battery model is analyzed and discussed.
- Accurate SoC and SoP joint estimator against varying health conditions is proposed.

## ARTICLE INFO

*Article history:*
Received 13 July 2013
Received in revised form
24 December 2013
Accepted 7 February 2014
Available online 6 March 2014

*Keywords:*
Adaptive extended Kalman filter
State-of-charge
State-of-power
Parameter update
Lithium-ion battery
Electrified vehicles

## ABSTRACT

Battery state-of-charge (SoC) and state-of-power capability (SoP) are two of the most significant decision factors for energy management system in electrified vehicles. This paper tries to make two contributions to the existing literature. (1) Based on the adaptive extended Kalman filter algorithm, a data-driven joint estimator for battery SoC and SoP against varying degradations has been developed. (2) To achieve accurate estimations of SoC and SoP in the whole calendar-life of battery, the need for model parameter updates with lowest computation burden has been discussed and studied. The robustness of the joint estimator against dynamic loading profiles and varying health conditions is evaluated. We subsequently used data from cells that have different aging levels to assess the robustness of the SoC and SoP estimation algorithm. The results show that battery SoP has close relationship with its aging levels. And the prediction precision would be significantly improved if recalibrating the parameter of battery capacity and resistance timely. What's more, the method reaches accuracies for new and aged battery cells in electrified vehicle applications of better than 97.5%.



## 1. Introduction

To address the two urgent tasks nowadays of protecting the environment and achieving energy sustainability, it is of strategic significance on a global scale to replace oil-dependent vehicles with electric vehicles. Battery, as important on-board electric energy storage, has been widely used in various electrified vehicles. The most important factor determining their successful commercialization is technologies safeguarding the reliable and safe battery operations. Battery management systems (BMS) have been designed to provide monitoring, diagnosis, and control functions to enhance the operations of battery. A critical function of BMS is to accurately estimate battery state-of-charge (SoC) and state-of-power capability (SoP) in real-time [1–3].

On one hand, the accurate battery SoC estimate is a key decision factor to manage batteries efficiently and to carry out the power distribution strategy in various electrified vehicles [4,5]. On the other hand, the accurate SoP estimate is critical in practical BMS applications since it is necessary to determine the available power in the moment to meet the acceleration, regenerative braking and gradient climbing power requirements without fear of over-charging or over-discharging. More importantly, accurate SoP estimates will be helpful to optimize the battery capacity and size and benefit the vehicle's general potency [6–8]. Therefore, to provide an efficient guarantee for the optimization of energy management system in electrified vehicles, a reliable SoC and SoP prediction algorithm is particularly necessary.

In terms of SoC estimation, a wide variety of methods has previously been summarized for constructing the SoC estimator, each one having its own advantage, as reviewed in Ref. [3]. Compared with direct measurement method, Coulomb counting method,

* Corresponding author. Tel./fax: +86 10 6891 4842.
*E-mail addresses:* rxiong6@gmail.com, rxiong@bit.edu.cn (R. Xiong).

http://dx.doi.org/10.1016/j.jpowsour.2014.02.095
0378-7753/

voltage and impedance measures based methods, filter algorithms or integrated algorithm based on multiple filters are attracting more attentions [9–18]. This is because that these kinds of approaches can hardly applied to electric vehicles directly, but the filters based approach can effectively avoid the problems from noise, inaccurate current sensor, accumulated round off error and so on. Ref. [9] used output injection-based PDE observer to predict the state of battery. Ref. [10] presented a comparative study among the nonlinear state observers and extended Kalman filters for predicting battery SoC. Ref. [11] used extended Kalman filters to predict battery SoC. Ref. [12] presented comprehensive unobservable model-based battery SoC, unknown nonlinearities, and state-of-health (SoH) estimation method. Refs. [13–18] presented several kinds of filters for estimating battery SoC. The above methods have achieved acceptable accuracy for battery SoC estimation. However, to achieve an optimized performance and longer calendar-life of a battery, an accurate battery SoP prediction method is necessary in addition to the knowledge of its SoC [19–21]. It is noted that any power/energy management system only focusing on the battery SoC is not reliable enough for electric vehicles. It needs to be adjusted to meet the requirements of battery SoP for long term objectives. Thus, compared with the research experience in battery SoC, the battery SoP estimation method is urgent needed.

In terms of SoP estimation, there are some methods have been presented to guarantee safe, efficient, and durable operations of the traction batteries under demanding driving conditions, which have been reviewed by Xiong, in Ref. [19]. The most commonly used approach is hybrid pulse power characterization (HPPC) method proposed by the Idaho National Engineering & Environmental Laboratory, which determines the static peak power in laboratory environments, but the estimates are over optimism. However, it is not suitable to estimate the continuous peak currents that are available for the next multi sampling intervals, additionally, the method neglects design limits like cell current, cell power or SoC [6]. As an improvement, the voltage-limited method was proposed by Plett [8]. However, these two *Rint* model-based methods hardly could simulate the relaxation effect performance and the estimates would diverge from the practical capability. To solve this problem, the authors in Ref. [7] proposed a dynamic electrochemical polarization battery model-based multi-parameter SoP estimation method. Then, to efficiently estimate the battery SoP under multiple sampling intervals, Ref. [21] has proposed a SoC and SoP joint estimator, which has achieved a good accuracy in real-time.

However, most of the above estimation methods were verified by the narrow set of scenarios of battery data, without exploring varying battery aging levels. In other words, the reliability of these estimation algorithms was not sufficiently assessed. For example, many estimation approaches mentioned above were evaluated under only one battery aging level. As a result, the performance of these algorithms against different health conditions was not adequately studied.

### 1.1. Contribution of the paper

In addition to the knowledge of SoC, the real-time SoP is also important for reliable battery operation in energy storage system, and these two states have close interactions in each other. Thus a data-driven SoC and SoP joint/dual estimator is urgently needed. However, battery performance is greatly restricted by its aging levels. As a consequence, little literature explores prediction methods for long term using. A key contribution of this study is to develop an accurate estimation method for battery SoC and SoP against varying health conditions. Thus the need of parameter update in real-time has been discussed and analyzed. What's more, the relationship between the battery parameter and its state has been evaluated by the data from cells that have different aging levels. The result is helpful for improving the performance of SoC and SoP joint estimator in its whole service period.

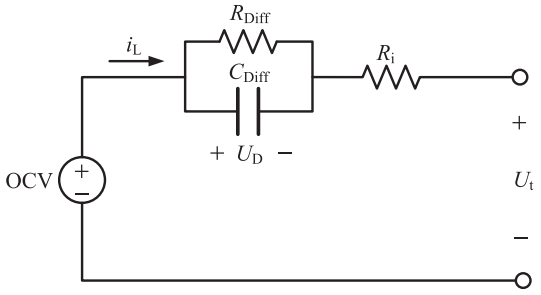


**Fig. 1.** The schematic diagram of the lumped parameter battery model.

### 1.2. Organization of the paper

A description of the lumped parameter battery model, battery experiments on several $LiFePO_4$ lithium-ion battery (LiB) cells and parameters identification method are given in Section 2. The data-driven SoC and SoP joint estimator is depicted in Section 3. The evaluation for the proposed battery parameters updating approach is illustrated in Section 4. Finally, conclusions are drawn in Section 5.

## 2. Modeling for the lithium-ion battery

### 2.1. The dynamic lumped parameter battery model

To achieve a reliable battery state estimation, an accurate battery model needs to be built at first. The lumped parameter battery model, which uses Nernst model to make the SoC as part of the model, is developed. The schematic of the battery model is shown in Fig. 1, it is very important to correctly identify the model parameter, including the open circuit voltage (OCV) which is used to describe the voltage source, series resistance ($R_i$) which is used to describe the electrical resistance of various battery components or with the accumulation and dissipation of charge in the electrical double layer, diffusion resistance ($R_{Diff}$) and diffusion capacitance ($C_{Diff}$) which consist of a RC network to describe the mass transport effects and dynamic voltage performances. The electrical behavior of the proposed model can be expressed by Eq. (1).

$$\begin{cases} \dot{U}_D = -\dfrac{1}{C_{Diff}R_{Diff}}U_D + \dfrac{1}{C_{Diff}}i_L \\ U_t = U_{oc} - U_D - i_L R_i \end{cases} \quad (1)$$

where $U_D$ is the polarization voltage across $C_{Diff}$, $U_t$ is the terminal voltage. Then the open circuit voltage $U_{oc}$ can be described as follows:

$$U_{oc} = K_0 + K_1 SoC + K_2/SoC + K_3 \ln SoC + K_4 \ln(1 - SoC) \quad (2)$$

where $K_i$ ($i = 0, 1, \ldots, 4$) are five polynomial involving different capacities and temperatures chosen to make the model fitting the test data accurately. However, the battery behavior of different temperatures will be discussed in our future work.

**Table 1**
Five aging levels of $LiFePO_4$ lithium-ion battery cells.

| Aging level | $SoH_1$ | $SoH_2$ | $SoH_3$ | $SoH_4$ | $SoH_5$ |
|---|---|---|---|---|---|
| Capacity/Ah | 12.5 | 11.76 | 11.4 | 10.7 | 9.6 |
| SoH | 1.04 | 0.98 | 0.95 | 0.89 | 0.80 |

### 2.2. The parameters identification method

In terms of the parameter tuning methods, the commonly used method is multiple linear regression method under the specified hybrid pulse power characterization (HPPC) data [22–24]. Anyway, it is hard to collect battery operating data in accordance with the format of the specified HPPC. As a result, this kind of parameter identification method hardly can be used to BMS directly. On the other hand, the time-series calculation based parameter identification methods have attracted more attentions, such as extended Kalman filter algorithm in Ref. [5], least square method with adaptive forgetting factor in Refs. [25,26]. Based on our previous experience in Ref. [6], the least square method has been employed to calibrate the parameter.

To identify the parameters of the proposed battery model, we need to calculate the parameter of Nernst model firstly. The parameters of $K_i$ can be solved by particle swarm optimization method with the experiment data among the OCV, SoC and capacity [27]. Then, to identify the other parameters, we need a time-series based discretization calculation for the battery model. Afterwards, from Ref. [6], a time-series format based discretization calculation of Eq. (1) can be rewritten as Eq. (3).

$$U_{t,k} = (1-a_1)U_{oc,k} + a_1 U_{t,k-1} + a_2 i_{L,k} + a_3 i_{L,k-1} \tag{3}$$

where, $U_{oc,k}$ and $U_{t,k}$ are the open circuit voltage and terminal voltage at the $k$th sampling time respectively, $i_{L,k}$ is the load current at the $k$th sampling time respectively (assumed positive for discharge, negative for charge). The model parameters can be deduced by the united equations of $a_1$, $a_2$ and $a_3$ in real-time. The related calculation equations are presented in Eq. (4).

To analyze the joint estimator against varying health conditions, five $LiFePO_4$ LiB cells with different capacities have been selected from the group of battery measured data. Table 1 shows that the capacity of the fresh cell is 12.5 Ah and a bit bigger than 12 Ah of its nominal value. It is noted that the SoH in Table 1 is defined to a ratio of battery capacity divided by its nominal value. Additional, the charge–discharge Coulomb efficiency is conducted and the result is shown in Table 2, which shows that the Coulomb efficiency has little difference with battery aging levels at the same temperature when operating currents are within ±2C. It is noted that, for the Li-ion prismatic cell with the nominal capacity of 12 Ah, a discharge current with a 1C rate is 12 A, which means that 1C current can discharge the battery cell from fully charged states to its lower cut off voltage with 1 h. The specific hybrid pulse test currents are shown in Fig. 2 including a sampling current curve in Fig. 2(a) and the whole current profiles in Fig. 2(b), where the sampling interval $\Delta t$ is 1 s. Based on Eqs. (3) and (4), we can estimate the model parameter with least square method in real-time.

Another OCV test is carried out to determine the relationship among SoC, OCV and capacities. The results show that the OCV values of $LiFePO_4$ LiB cell have smaller interaction with its SoH except the top and bottom of the SoC. It is because that $LiFePO_4$ LiB cell has a flat OCV behavior, which results in smaller divergence in battery voltage under different SoC. As a result, it is hard to accurately project the SoC trajectory for filters based SoC estimation method. To overcome the problem, the enhanced OCV analytic equation has been developed and used to describe the OCV behavior of $LiFePO_4$ LiB cell. Herein we use the data of fresh LiB cell to describe the relationship between the OCV and SoC. Then we can solve the parameter in Eq. (2) for OCV behavior.

$$\begin{cases} a_1 = -\dfrac{1-2R_{Diff}C_{Diff}}{1+2R_{Diff}C_{Diff}},\ a_2 = -\dfrac{R_i+R_{Diff}+2R_iR_{Diff}C_{Diff}}{1+2R_{Diff}C_{Diff}},\ a_3 = -\dfrac{R_i+R_{Diff}-2R_iR_{Diff}C_{Diff}}{1+2R_{Diff}C_{Diff}} \\ R_i = \dfrac{a_3-a_2}{1+a_1},\ R_{Diff} = \dfrac{2(a_3+a_1a_2)}{a_1^2-1},\ C_{Diff} = \dfrac{-1}{4}\dfrac{(a_1+1)^2}{a_3+a_1a_2} \end{cases} \tag{4}$$

### 2.3. Battery experiments

The experiment data used for this study are acquired through the battery test bench set up in Ref. [2], which consisted of a battery testing system (Arbin BT2000), a thermal chamber for environment control, a computer for the human–machine interface and experimental data storage and the LiB cells or LiB pack. The Arbin BT2000 has eight independent channels which can charge or discharge eight battery cells independently according to the designed profile with a maximum voltage of 5 V and a maximum current of 100 A in three scales (1 A/10 A/100 A). The measurement errors of the current and voltage sensors are less than 0.1%. The experiment procedure starts with a series of characterization tests (which consists of a maximum available capacity test using current rate ½C, a hybrid pulse test, OCV-SoC test and loading profiles test) conducted at constant temperature of 25 °C. The Urban Dynamometer Driving Schedule (UDDS) loading profiles are used to verify and evaluate the performance of the proposed parameter updating method based SoC and SoP joint estimator.

$$\begin{aligned} U_{oc} = {} & 3.380 - 0.0425 \times SoC + 2.236 \times 10^{-5}/SoC \\ & + 0.0735 \ln SoC - 1.35 \times 10^{-3} \ln(1 - SoC) \end{aligned} \tag{5}$$

In addition to the numerical study using synthetic data, we also conducted the UDDS cycle test to verify the effectiveness of the proposed approach. Since the battery cannot withstand high current pulse of a typical HEV cycle, the current rate of UDDS profile in this study has been scaled down to ±2C. The discharging process was designed to excite the entire SoC range (100–10%) of the UDDS test. And it can collect the UDDS profiles data under different SoC levels separated by a small gap (about 3% for fresh state). The loading profiles are composed with 30 cycles, separated by 20 A constant current discharge and 5 min rest. This test profile resulted in the spread of SoC over the 100–10% range. The current curve for one UDDS cycle is shown in Fig. 3(a), and the SoC profile for entire UDDS cycles is plotted in Fig. 3(b), where the battery experiences a SoC increase by about 3% for fresh cell during each

**Table 2**
Coulomb efficiency data.

| Current | −4C | −2C | −1.5C | −1C | −1/3C | 1/3C | 1C | 1.5C | 2C | 4C |
|---|---|---|---|---|---|---|---|---|---|---|
| Efficiency | 0.955 | 0.985 | 0.992 | 0.996 | 1 | 1 | 0.998 | 0.995 | 0.990 | 0.975 |

UDDS cycle which combines constant current discharge. In all cases, "true" SoC was calculated from the Arbin data log using Coulomb counting on measured data, and the "true" SoC is only approximately accurate since there is a current sensor error and which is accumulated over time when using coulomb counting to calculate the SoC.

## 3. Joint estimator for battery SoC and SoP

Based on our previous experience in SoC estimation [3,5], the key objective of this study is to develop an accurate estimation method for battery SoC and SoP against varying health conditions. Thus we need to find the relationship between the battery parameter and varying health conditions and carry out the parameter update strategy for improving the control accuracy of SoC and SoP with minimum calculation cost.

To employ the AEKF algorithm for battery SoC and SoP joint predicting, we should have a system model in a discrete state-space. Specifically, we assume a very general framework for discrete-time lumped dynamic systems [28].

$$\mathbf{X}_k = \begin{pmatrix} U_{\mathrm{Diff},k} \\ \mathrm{SoC}_k \end{pmatrix},\quad \mathbf{Y}_k = U_{\mathrm{t},k},\quad \mathbf{u}_k = i_{\mathrm{L},k},\quad \mathbf{A} = \begin{pmatrix} \exp(-\Delta t/\tau) & 0 \\ 0 & 1 \end{pmatrix},\quad \mathbf{D} = [-R_{\mathrm{i}}]$$
$$\mathbf{B} = \begin{pmatrix} R_{\mathrm{Diff}}(1-\exp(-\Delta t/\tau)) \\ \dfrac{\eta_{\mathrm{i}}\Delta t}{C_{\mathrm{n}}} \end{pmatrix},\quad \mathbf{C} = \left.\frac{\partial U_{\mathrm{t}}}{\partial \mathbf{X}}\right|_{\mathbf{X}=\widehat{\mathbf{X}}_{k+1}^{-}} = \left[-1 \quad \left.\frac{\mathrm{d}U_{\mathrm{oc}}(z)}{\mathrm{d}z}\right|_{z=z_{k+1}^{-}}\right], \tag{11}$$

$$\mathbf{X}_{k+1} = \mathbf{A}_k\mathbf{X}_k + \mathbf{B}_k\mathbf{u}_k + \omega_k \tag{6}$$

$$\mathbf{Y}_{k+1} = \mathbf{C}_k\mathbf{X}_{k+1} + \mathbf{D}_k\mathbf{u}_{k+1} + \upsilon_k \tag{7}$$

where $\mathbf{X}_k$ is the system state vector at the $k$th sampling time, which represents the total effect of system inputs $\mathbf{u}_k$ on the present system operation, such as SoC. $\omega_k$ is the unmeasured "process noise" that affects the system state and $\upsilon_k$ is the measurement noise which does not affect the system state, but can be reflected in the system output estimates $\mathbf{Y}_k$. And $\omega_k$ is assumed to be Gaussian white noise with zero mean and covariance $\mathbf{Q}_k$; $\upsilon_k$ is assumed to be Gaussian white noise with zero mean and covariance $\mathbf{R}_k$. The matrices $\mathbf{A}_k$, $\mathbf{B}_k$, $\mathbf{C}_k$ and $\mathbf{D}_k$ describe the dynamics of the system.

### 3.1. SoC estimator using the AEKF algorithm

According to the SoC definition, the battery SoC is the ratio of the remaining capacity to the available capacity (in ampere hour):

$$z_k = z_0 - \int_0^k \eta_{\mathrm{i}} i_{\mathrm{L},t}\mathrm{d}t/C_{\mathrm{n}} \tag{8}$$

It is noted that, we use the maximum available capacity $C_{\mathrm{n}}$ to calculate the SoC, specifically for fresh cell the $C_{\mathrm{n}}$ is 12.5 Ah, instead of its nominal value. Since the nominal capacity is a constant value and it is not reliable when the operating conditions has been changed. Then,

$$z_k = z_{k-1} - \eta_i I_{\mathrm{L},k}\Delta t/C_{\mathrm{n}} \tag{9}$$

To perform the battery SoC prediction, we should have a discrete state-space model to describe the dynamics of the battery model. Transform Eq. (1) to a discrete system:

$$\begin{cases} U_{\mathrm{Diff},k+1} = U_{\mathrm{Diff},k}\exp(-\Delta t/\tau) + i_{\mathrm{L},k}R_{\mathrm{Diff}}(1-\exp(-\Delta t/\tau)) \\ U_{\mathrm{t},k+1} = U_{\mathrm{oc},k+1} - i_{\mathrm{L},k}R_{\mathrm{i}} - U_{\mathrm{Diff},k+1} \end{cases} \tag{10}$$

where $\tau$ ($=R_{\mathrm{Diff}} \times C_{\mathrm{Diff}}$) is the time constant. The state and observation function are expressed as:

where, $dU_{\mathrm{oc}}/dz = K_1 - K_2/z^2 + K_3/z - K_4/(1-z)$ calculated from Eq. (2).

Thus the battery SoC can be estimated in accordance with the operating process of AEKF algorithm shown in Table 3.

### 3.2. Battery SoP estimator

The input of the system is assumed to constant between the $k$th sampling time $t_k$ and the $(k+L)$th sampling time $t_{k+L}$, it is expressed by $\mathbf{u}_{k+L} = \mathbf{u}_k$ within the sampling intervals of $L \times \Delta t$. Then, we use battery model to predict battery voltage at the $(k+L)$ th sampling time by:

$$\begin{cases} \mathbf{X}_{k+L} = \mathbf{A}\mathbf{X}_{k+L-1} + \mathbf{B}\mathbf{u}_{k+L-1} \\ \mathbf{Y}_{k+L} = \mathbf{C}\mathbf{X}_{k+L} + \mathbf{D}\mathbf{u}_{k+L-1} \end{cases} \tag{20}$$

Assuming that the input keeps constant over the entire prediction horizon (from time $t_k$ to $t_{k+L}$), from Eqs. (6) and (20), we have:

$$\mathbf{X}_{k+L} = \mathbf{A}^L\mathbf{X}_k + \left(\sum_{j=0}^{L-1}\mathbf{A}^{L-1-j}\mathbf{B}\right)\mathbf{u}_k \tag{21}$$

To find the minimum charging current $I_{\mathrm{min},L}^{\mathrm{chg,dd}}$, the output of the system should satisfy the following equation:

$$U_{\mathrm{oc}}(z_{k+L}) - U_{\mathrm{Diff},k}\left(\exp\left(\frac{-\Delta t}{\tau}\right)\right)^L - I_{\mathrm{min},L}^{\mathrm{chg,dd}}\left(R_{\mathrm{i}} + R_{\mathrm{Diff}}\left(1-\exp\left(\frac{-\Delta t}{\tau}\right)\right)\sum_{j=0}^{L-1}\left(\exp\left(\frac{-\Delta t}{\tau}\right)\right)^{L-1-j}\right) - U_{\mathrm{t,max}} = 0 \tag{22}$$

where the SoC is denoted by $z$, $z_k$ is the SoC at the $k$th sampling time, $z_0$ is the initial SoC, $I_{\mathrm{L},t}$ is the instantaneous load current. The $\eta_{\mathrm{i}}$ is Coulomb efficiency is used to calculate the capacity loss at different operating operations.

where $U_{\mathrm{t,max}}$ and $U_{\mathrm{t,min}}$ are the design limits of the upper and lower cut off voltage respectively. To find the maximum discharging current $I_{\mathrm{min},L}^{\mathrm{dis,dd}}$, the output of the system should satisfy the following equation:

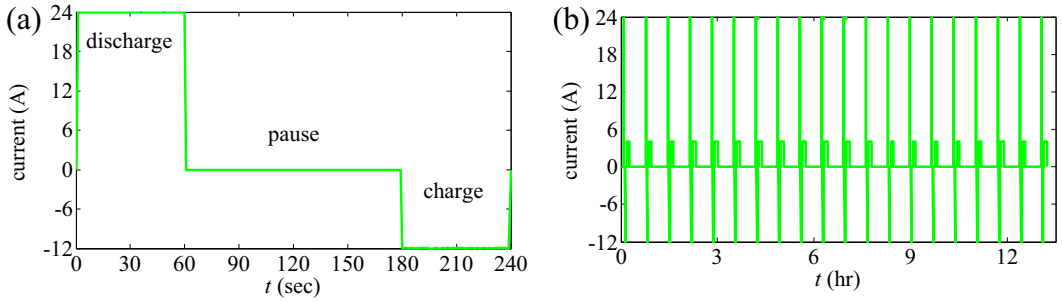


**Fig. 2.** Hybrid pulse test. (a) Current profile of one hybrid pulse. (b) Current profiles.

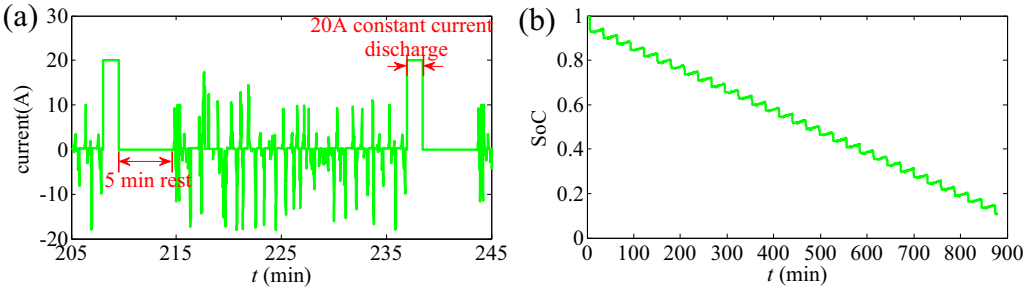


**Fig. 3.** Plots showing SoC versus time and current versus time for UDDS battery test (fresh state). Current for one UDDS cycle is shown in (a); SoC for the entire test is shown in (b).

$$U_{\mathrm{oc}}(z_{k+L}) - U_{\mathrm{Diff},k}\left(\exp\left(\frac{-\Delta t}{\tau}\right)\right)^{L} - I_{\mathrm{max},L}^{\mathrm{dis,dd}}\left(R_{\mathrm{i}} + R_{\mathrm{Diff}}\left(1 - \exp\left(\frac{-\Delta t}{\tau}\right)\right)\sum_{j=0}^{L-1}\left(\exp\left(\frac{-\Delta t}{\tau}\right)\right)^{L-1-j}\right) - U_{\mathrm{t,min}} = 0 \tag{23}$$

Then, we can get the computational approach to predict peak current from the $k$th sampling time to the $(k+L)$th sampling time by:

$$\begin{cases} I_{\mathrm{max},L}^{\mathrm{dis,dd}} = \dfrac{U_{\mathrm{oc}}(z_k) - U_{\mathrm{Diff},k}\left(\exp\left(\frac{-\Delta t}{\tau}\right)\right)^{L} - U_{\mathrm{t,min}}}{\frac{\eta_{\mathrm{i}} L \Delta t}{C_{\mathrm{n}}}\left.\frac{\mathrm{d}U_{\mathrm{oc}}(z)}{\mathrm{d}z}\right|_{z_k} + R_{\mathrm{Diff}}\left(1 - \exp\left(\frac{-\Delta t}{\tau}\right)\right)\sum_{j=0}^{L-1}\left(\exp\left(\frac{-\Delta t}{\tau}\right)\right)^{L-1-j} + R_{\mathrm{i}}} \\ I_{\mathrm{min},L}^{\mathrm{chg,dd}} = \dfrac{U_{\mathrm{oc}}(z_k) - U_{\mathrm{Diff},k}\left(\exp\left(\frac{-\Delta t}{\tau}\right)\right)^{L} - U_{\mathrm{t,max}}}{\frac{\eta_{\mathrm{i}} L \Delta t}{C_{\mathrm{n}}}\left.\frac{\mathrm{d}U_{\mathrm{oc}}(z)}{\mathrm{d}z}\right|_{z_k} + R_{\mathrm{Diff}}\left(1 - \exp\left(\frac{-\Delta t}{\tau}\right)\right)\sum_{j=0}^{L-1}\left(\exp\left(\frac{-\Delta t}{\tau}\right)\right)^{L-1-j} + R_{\mathrm{i}}} \end{cases} \tag{24}$$

In addition to the constraint from battery voltage, the SoC is another necessary decision factor for predicting battery power. For instance, when actual battery SoC closes to its lower design limit—$z_{\min}$,, we should reduce the discharge current and maximize the charge current Otherwise, the battery will result in over-discharged. On the other hand, we should reduce its charge current and maximize its discharge current when actual SoC closes to its higher design limits $z_{\max}$, otherwise, the battery will result in over-charged. This is the basic principle for the SoP prediction with the constraint of battery SoC. The computational equation and related description is presented in Eq. (25). It is derived from Eq. (9).

**Table 3**
Algorithm of adaptive extended Kalman filtering.

| | |
|---|---|
| **Step I: Initialization** | |
| For $k$=0, set: $\widehat{\mathbf{X}}_0^+ = E[\mathrm{X}_0]$, $\mathbf{P}_0^+ = E[(\mathrm{X}_0 - \widehat{\mathbf{X}}_0^+)(\mathrm{X}_0 - \widehat{\mathbf{X}}_0^+)^{\mathrm{T}}]$, $\mathbf{q}_0, \mathbf{r}_0$ | (12) |
| **Step II: Prior estimation (forecast)** ( For $k$ = 1,2,……, compute | |
| State estimate time update $\widehat{\mathbf{X}}_k^- = \mathbf{A}_k\widehat{\mathbf{X}}_{k-1}^+ + \mathbf{B}_k\mathbf{u}_k$ | (13) |
| Error covariance time update: $\mathbf{P}_k^- = \mathbf{A}_k\mathbf{P}_{k-1}\mathbf{A}_k^{\mathrm{T}} + \mathbf{q}_{k-1}$ | (14) |
| **Step III: Posterior estimation (correction)** - For $k$ = 1,2,……, compute | |
| Error innovation: $\mathbf{e}_k = \mathbf{Y}_k - \mathbf{C}_k\widehat{\mathbf{X}}_k^- - \mathbf{D}_k\mathbf{u}_k$ | (15) |
| Kalman gain matrix: $\mathbf{K}_k = \mathbf{P}_k^-\mathbf{C}_k^{\mathrm{T}}(\mathbf{C}_k\mathbf{P}_k^-\mathbf{C}_k^{\mathrm{T}} + \mathbf{r}_{k-1})^{-1}$ | (16) |
| Adaptive covariance matching: $\mathbf{H}_k = \frac{1}{M}\sum_{i=k-M+1}^{k}\mathbf{e}_k\mathbf{e}_k^{\mathrm{T}}$, $\mathbf{r}_k = \mathbf{H}_k - \mathbf{C}_k\mathbf{P}_k^-\mathbf{C}_k^{\mathrm{T}}$, $\mathbf{q}_k = \mathbf{K}_k\mathbf{H}_k\mathbf{K}_k^{\mathrm{T}}$ | (17) |
| State estimate measurement update: $\widehat{\mathbf{X}}_k^+ = \widehat{\mathbf{X}}_k^- + \mathbf{K}_k\mathbf{e}_k$ | (18) |
| Error covariance measurement update: $\mathbf{P}_k^+ = (\mathbf{I} - \mathbf{K}_k\mathbf{C}_k)\mathbf{P}_k^-$ | (19) |

Where $\mathbf{H}_k$ is the innovation covariance matrix based on the innovation sequence $\mathbf{e}_k$ inside a moving estimation window of size $M$ at the $k$th sampling time, $\mathbf{K}_k$ is Kalman gain matrix at the $k$th sampling time; $\widehat{\mathbf{X}}_k^-$ is the *priori* estimate of $\mathbf{X}_k$ *before* the measurement $\mathbf{Y}_k$ is taken into account, $\widehat{\mathbf{X}}_k^+$ is the estimate of $\mathbf{X}_k$ after the measurement $\mathbf{Y}_k$ is taken into account, which is called *posteriori* estimate; $U_{\mathrm{t},k}$ and $\widehat{U}_{\mathrm{t},k}$ are the terminal voltage measured and estimated by the battery model at the $k$th sampling time respectively.

$$\begin{cases} I_{\min,L}^{\mathrm{chg,soc}} = \dfrac{z_k - z_{\max}}{\eta_i L \Delta t / C_n} \\ I_{\max,L}^{\mathrm{dis,soc}} = \dfrac{z_k - z_{\min}}{\eta_i L \Delta t / C_n} \end{cases} \tag{25}$$

where $I_{\min,L}^{\mathrm{chg,SoC}}$ and $I_{\max,L}^{\mathrm{dis,SoC}}$ are the minimum charge current and maximum discharge current between the $L \times \Delta t$ sampling intervals under the SoC design limits. Once the current design limit is calculated, the peak currents with all limits enforced are calculated as:

$$\begin{cases} I_{\max}^{\mathrm{dis}} = \min\left(I_{\max}, I_{\max,L}^{\mathrm{dis,SoC}}, I_{\max,L}^{\mathrm{dis,dd}}\right) \\ I_{\min}^{\mathrm{chg}} = \max\left(I_{\min}, I_{\min,L}^{\mathrm{chg,SoC}}, I_{\min,L}^{\mathrm{chg,dd}}\right) \end{cases} \tag{26}$$

where $I_{\max}$ and $I_{\min}$ are design limits for the maximum discharge current and minimum charge current respectively. $I_{\min}^{\mathrm{chg}}$ and $I_{\max}^{\mathrm{dis}}$ are the minimum charge current and maximum discharges current respectively with all limits enforced. Then the peak power capability estimation based on the dynamic model-based can be calculated as follows:

$$\begin{cases} P_{\min}^{\mathrm{chg}} = \max\left(P_{\min}, U_{t,k+L} I_{\min}^{\mathrm{chg}}\right) \\ P_{\max}^{\mathrm{dis}} = \min\left(P_{\max}, U_{t,k+L} I_{\max}^{\mathrm{dis}}\right) \end{cases} \tag{27}$$

where $P_{\max}$, $P_{\min}$ are the battery's power design limits, $P_{\max}$ denotes the peak discharge power and $P_{\min}$ denotes the peak charge power of its design limits respectively.

Then we can get the computational approach for peak power estimation when we take the terminal voltage calculation equation as follows.

$$\begin{aligned} U_{t,k+1} = {} & U_{oc}\left(z_k - \frac{\eta_i i_{L,k+1} L \Delta t}{C_n}\right) - U_{\mathrm{Diff},k} \exp\left(\frac{-\Delta t}{\tau}\right) \\ & - i_{L,k}\left(R_i + R_{\mathrm{Diff}}\left(1 - \exp\left(\frac{-\Delta t}{\tau}\right)\right)\right) \end{aligned} \tag{28}$$

Then,

$$\begin{cases} P_{\min}^{\mathrm{chg}} \approx \max\left\{ P_{\min}, \left( \begin{array}{l} U_{oc}(z_k) - U_{\mathrm{Diff},k}\left(\exp\left(\frac{-\Delta t}{\tau}\right)\right)^{L} - I_{\min}^{\mathrm{chg}}\left(\frac{L\eta_i \Delta t}{C_a} \frac{dU_{oc}}{dz}\middle| z_k \right. \\ \\ + R_i + R_{\mathrm{Diff}}\left(1 - \exp\left(\frac{-\Delta t}{\tau}\right)\right) \sum_{j=0}^{L-1} \left(\exp\left(\frac{-\Delta t}{\tau}\right)\right)^{L-1-j} \end{array} \right) \times I_{\min}^{\mathrm{chg}} \right\} \\ P_{\max}^{\mathrm{dis}} \approx \min\left\{ P_{\max}, \left( \begin{array}{l} U_{oc}(z_k) - U_{\mathrm{Diff},k}\left(\exp\left(\frac{-\Delta t}{\tau}\right)\right)^{L} - I_{\max}^{\mathrm{dis}}\left(\frac{L\eta_i \Delta t}{C_a} \frac{dU_{oc}}{dz}\middle| z_k \right. \\ \\ + R_i + R_{\mathrm{Diff}}\left(1 - \exp\left(\frac{-\Delta t}{\tau}\right)\right) \sum_{j=0}^{L-1} \left(\exp\left(\frac{-\Delta t}{\tau}\right)\right)^{L-1-j} \end{array} \right) \times I_{\max}^{\mathrm{dis}} \right\} \end{cases} \tag{29}$$

### 3.3. The data-driven joint estimator for battery SoC and SoP

In order to use a data-driven joint estimator for battery SoC and SoP, a very general framework for online estimation is presented in Fig. 4.

The operating process of the flowchart can be divided into four parts in orderly.

- **Step 1** – On-board data measurement. After the discharge and charge current profiles are loaded on LiB cells, the real-time currents and voltages are measured through their sensors.
- **Step 2** – Model parameter update. With the measured data, we can update the model parameters with the method presented in Ref. [6]. Firstly, with the prior SoC estimate, the OCV can be updated with Eq. (2), the other parameter can be updated by time-series calculation method in accordance with Eq. (4).
- **Step 3** – Adaptive SoC estimator. After the parameter identification, the voltage error and updated parameters are transmitted to the SoC estimator. The AEKF algorithm adjusts the SoC to update the OCV to optimize the model output voltage for minimizing the voltage error. After several computations, the voltage error will be greatly reduced and converged to a minimal value, and the SoC will converge to its reference trajectory finally. Afterwards, the SoC estimate is used to update the battery OCV parameter for the prediction at next sampling interval. Lastly, the accurate estimate of SoC and $U_{\mathrm{Diff}}$ will be transmitted to SoP estimator.
- **Step 4** – SoP estimator. With the SoC estimates, we can calculate the peak currents with voltage-limited method in Eq. (24) and SoC-limited method in Eq. (25). When taking the consideration of the design limits of current, voltage and power, we can calculate the SoP estimates with Eqs. (27) and (29). Lastly, we can get the accurate joint estimation for battery SoC and SoP.

## 4. Verification and discussion

This section firstly evaluates the estimation accuracy of the joint estimator under UDDS profiles of the fresh state. To discuss and analyze the performance of the joint estimator against varying health conditions, the parameter updating method has proposed and developed in the later section.

### 4.1. Verification with fresh cell

Before the verification, we should give the design limits for battery SoC. It is noted that the upper and lower cut off voltage, power and current are limited by the battery manufacturers. It is obvious that for different control strategies, the SoC threshold is different. The threshold for this study is presented in Table 4.

Where the peak current and peak power design limits are restricted for continuous power, therefore for a short time which less than 1 s, the peak currents and powers will be much bigger than the values present in the Table 4. It is more than120/−96 A and

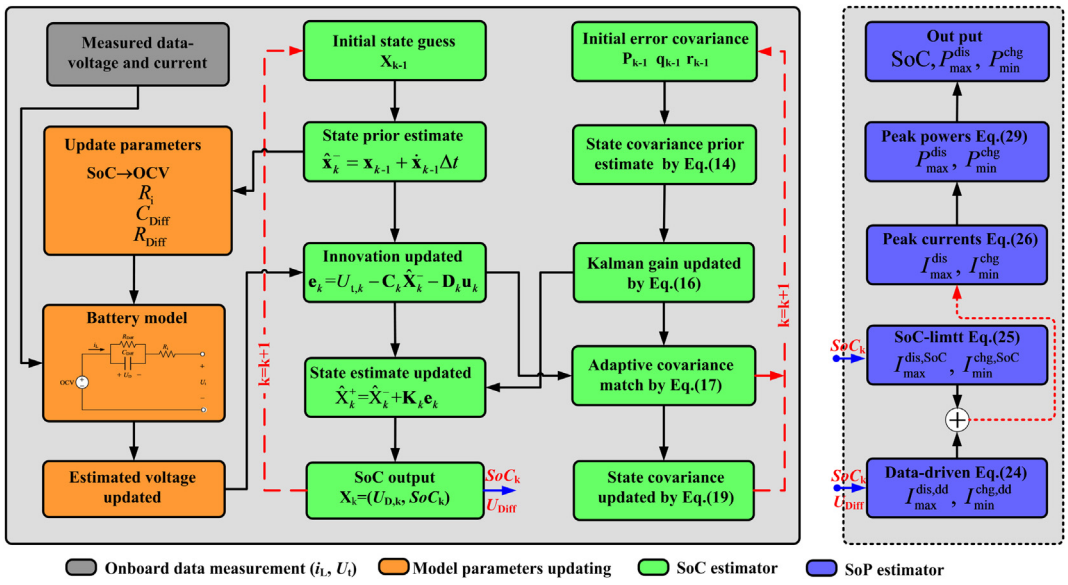


**Fig. 4.** The flowchart of the joint estimation estimator for battery SoC and SoP using AEKF algorithm.

450/−300 W. These thresholds are set by the battery manufacturer for avoiding excessive discharge rates that would damage the battery or reduce its capacity. Along with the maximum continuous power of the motor, this threshold defines the maximum available sustainable speed and acceleration of the electrified vehicle.

The SoC estimation has conducted and its results are plotted in Fig. 5, where the initial state of the estimator is incorrectly initialized to 0.5 and 0.9.

From Fig. 5(a), we find that the estimated terminal voltage tracks the references accurately. The predicted inaccuracy plotted in Fig. 5(b) indicates that the voltage error is less than 50 mV. It is because that the AEKF algorithm based method can precisely project the state and timely adjust the Kalman gain matrix according to the terminal voltage error between the measured data and the estimated values. The evaluation results of SoC are shown in Fig. 5(c). From Fig. 5(c), we find that the SoC estimation results with the two erroneous initial SoCs converge to the same reference. The zoom figure enlightens the performance of the AEKF-based SoC estimator, which indicates this estimator can ensure the stable SoC estimation accuracy after several sampling intervals for its convergence process. To make the evaluation more clarity, we plot the SoC estimation error in Fig. 5(d), which further proves the accuracy and performance of the proposed SoC estimator. The precision of the SoC estimation is helpful for the reliable SoP estimation.

In addition to the SoC estimation, we also have predicted the real-time SoP for instantaneous and 30 s continuance sampling intervals, the results are plotted in Fig. 6.

From Fig. 6, we find that the estimate of battery SoP has strong relationship with the required output sampling intervals width. Specifically, bigger sampling intervals width will result in smaller SoP estimate. It also indicates that the continuous output power is much smaller than the instantaneous estimates. As a result, the design thresholds from the battery manufacturers' manual are not accurate enough for long term operating. Thus, we should calculate it in accordance with the energy management strategies in electrified vehicles. Fig. 6(a) shows that the absolute value of SoP is very small when battery SoC closes to its higher threshold, but the peak discharge current is very big. This is because that the battery with higher SoC will result in over-charged and has big capable for discharge operation. In a similar way, when battery SoC closes to its lower threshold, the discharge current will be very small, but the absolute value of peak charge current is quite big. From Fig. 6(b), we find that the peak discharge current is big when battery SoC is big, and the peak discharge current closes to zero when SoC reaches its lower threshold. From Fig. 6(c) and (d), we find that the SoP estimates have the similar behavior as the peak current.

The above discussion shows that the SoC estimation error is less than 0.01 even provided with big erroneous initial state of the estimator. However, all the above results are got on the basis of the fresh cell. For a reliable state estimator, the results should be verified considering the various health conditions of a battery.

**Table 4**
Parameter threshold for SoP estimation (30 s).

| Parameters | Maximum value | Minimum value |
|---|---|---|
| SoC ($z_{max}$, $z_{min}$) | 1.0 | 0.20 |
| $U_t$ ($U_{t,max}$, $U_{t,min}$)/V | 3.65 | 2.5 |
| $I_L$ ($I_{max}$, $I_{min}$)/A | 96 | −72 |
| $P$ ($P_{max}$, $P_{min}$)/W | 300 | −200 |

### 4.2. Verification with various health condition cells

To verify and evaluate the performance of the joint estimator against different battery aging levels, firstly we will discuss the performance of the SoC estimator, which is the base of the joint estimator. Then we will discuss the updating strategy of battery parameter. Lastly, we will evaluate the performance of the joint estimator against various health conditions. It is noted that we name the model built with the data of fresh cell (at $SoH_1$ aging level) with **nominal** model.

#### 4.2.1. SoC estimation without parameter update

This section discusses the estimation accuracy of the SoC estimator without parameter updating. The analysis results for the absolute value of the terminal voltage and SoC error are presented in Table 5, and the initial SoC is incorrectly initialized to 0.5.

From Table 5, we find that the maximum voltage error is less than 2% of its nominal voltage (nominal voltage is 3.2 V) for the fresh cell. What's more, its mean error and standard deviation are

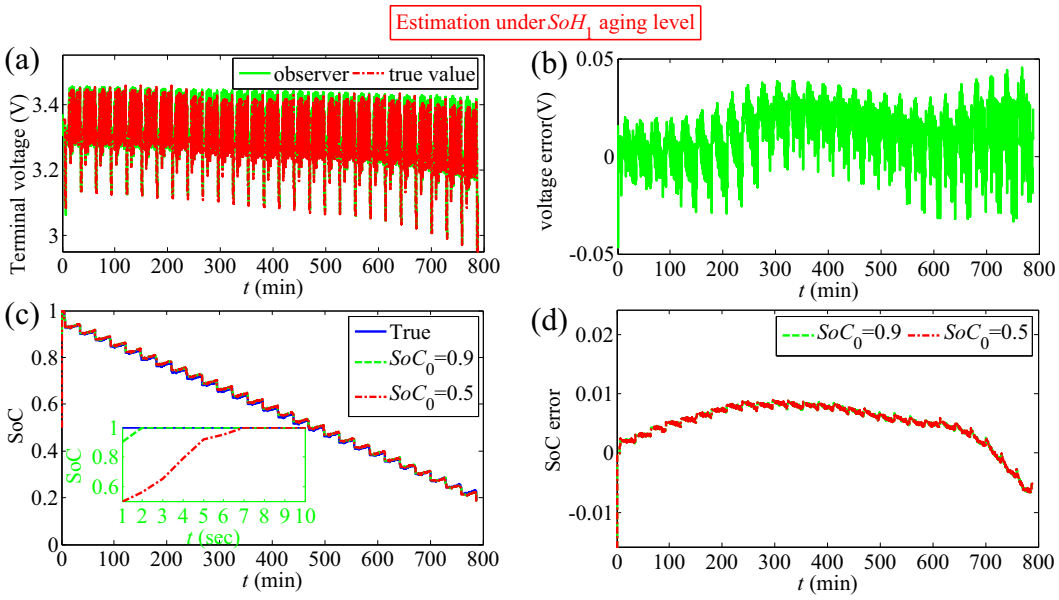


**Fig. 5.** AEKF-based SoC estimation results: (a) terminal voltage; (b) voltage estimation error; (c) SoC estimation with $SoC_0 = 0.9$ and $SoC_0 = 0.5$; (d) SoC estimation error for (c).

very small. The relevant description is plotted in Fig. 5(a) and (b). Table 5 shows that the prediction performance has great relationship with its health conditions. For instance, the maximum voltage error will increase to 0.237 V from 0.0464 V if using the **nominal** model. Battery parameter degrades as its aging, which results in the gradually increased error. On the other hand, Table 5 indicates that the SoC estimation error will reach to 0.684 if using the **nominal** model. However, the estimation performance under the UDDS datasheet in level 01 ($SoH_1$) is desirable. Thus, as the aging of the battery, the voltage and SoC estimation error will become bigger and bigger if without the update for battery parameter timely.

Therefore, it is very important to update the model parameter of battery for a reliable state estimation in its whole service period.

*4.2.2. SoC estimation with parameter update*

This section discusses the estimation accuracy of SoC with parameters updating operation. Although the **nominal** model is built under the datasheet of fresh cell, its parameters will be update with the archived data in a period of time to improve its accuracy. The analysis results for the absolute value of the terminal voltage and SoC error with capacity parameter update are shown in Table 6, where the initial SoC is incorrectly initialized to 0.5. Table 6 shows that the voltage errors are smaller than the estimation without parameter updating shown in Table 5. But the voltage estimates are not accurate enough for state estimation. For the datasheet under $SoH_2$ aging level, the maximum error is less than 5% of its nominal voltage, but for $SoH_3$ aging level it has exceeded to 5%, and for $SoH_4$

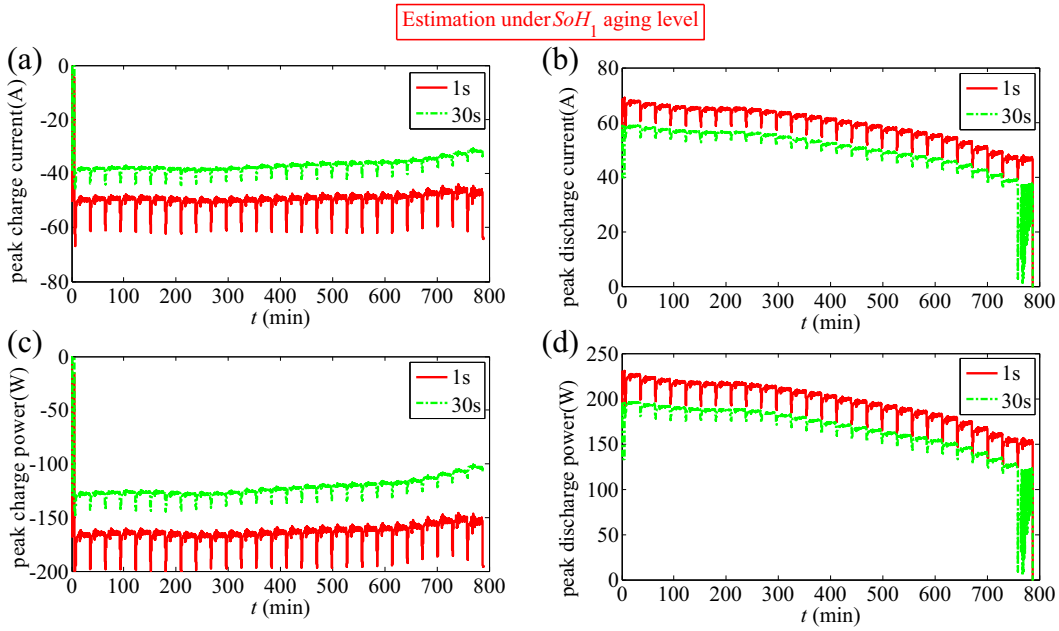


**Fig. 6.** The SoP estimation results: (a) peak charge current; (b) peak discharge current; (c) peak charge power; (d) peak discharge power.

**Table 5**
Voltage and SoC error analysis for the model without parameter updating.

| Error | $SoH_1$ | $SoH_2$ | $SoH_3$ | $SoH_4$ | $SoH_5$ |
|---|---|---|---|---|---|
| Maximum/V (voltage) | 0.0464 | 0.0500 | 0.0845 | 0.2155 | 0.2374 |
| Mean/V (voltage) | 0.0120 | 0.0136 | 0.0241 | 0.0268 | 0.0388 |
| Standard deviation/V (voltage) | 0.0082 | 0.0088 | 0.0147 | 0.0222 | 0.0329 |
| Maximum/after 10 s (SoC) | 0.5/0.009 | 0.5/0.025 | 0.5/0.082 | 0.5/0.130 | 0.5/0.684 |
| Mean (SoC) | 0.0056 | 0.0121 | 0.0403 | 0.0610 | 0.3432 |
| Standard deviation (SoC) | 0.0042 | 0.0046 | 0.0151 | 0.0254 | 0.1767 |

**Table 6**
Voltage error analysis for the model with capacity updating.

| Error | $SoH_2$ | $SoH_3$ | $SoH_4$ | $SoH_5$ |
|---|---|---|---|---|
| Maximum/V (voltage) | 0.0492 | 0.0661 | 0.1449 | 0.1494 |
| Mean/V (voltage) | 0.0111 | 0.0178 | 0.019 | 0.0291 |
| Standard deviation/V (voltage) | 0.0085 | 0.0124 | 0.0177 | 0.0287 |
| Maximum/after 10 s (SoC) | 0.5/0.014 | 0.5/0.022 | 0.5/0.032 | 0.5/0.041 |
| Mean (SoC) | 0.0071 | 0.0092 | 0.0157 | 0.0123 |
| Standard deviation (SoC) | 0.009 | 0.0102 | 0.0108 | 0.0115 |

**Table 7**
Terminal voltage error analysis for the model with capacity and $R_i$ updating.

| Voltage error | $SoH_2$ | $SoH_3$ | $SoH_4$ | $SoH_5$ |
|---|---|---|---|---|
| Maximum/V (voltage) | 0.0464 | 0.0484 | 0.0626 | 0.0608 |
| Mean/V (voltage) | 0.011 | 0.0163 | 0.0154 | 0.0205 |
| Standard deviation/V (voltage) | 0.0077 | 0.0097 | 0.0104 | 0.0110 |
| Maximum/after 10 s (SoC) | 0.5/0.011 | 0.5/0.016 | 0.5/0.021 | 0.5/0.024 |
| Mean (SoC) | 0.0062 | 0.0085 | 0.0106 | 0.0122 |
| Standard deviation (SoC) | 0.0081 | 0.0096 | 0.0098 | 0.0104 |

and $SoH_5$ aging levels the maximum errors are more than 10%. It can be concluded that the model only updating the capacity is not reliable enough for practical application. On the other hand, Table 6 shows that the SoC errors are much smaller than the estimation without parameter updating shown in Table 5. More importantly, all the SoC estimation errors are less than 0.05. Especially for the battery at $SoH_5$ aging level, the maximum SoC estimation error is 0.041, and the mean error and standard deviation are 0.0123 and 0.115 respectively, which is acceptance for SoC estimation. Therefore, the battery model only updating battery capacity is acceptance for SoC estimation against varying aging levels.

Based on the above analysis, we can conclude that if only updates the capacity parameter of the battery, the voltage prediction error hardly can be controlled to an acceptable level. As a consequence, the ohmic resistance $R_i$ should be added to the updating list of battery parameter.

The analysis results for the absolute value of the voltage and SoC error with capacity and $R_i$ parameters update are shown in Table 7

Table 7 shows that both the voltage and SoC estimation errors are much smaller than the estimation result without parameter updating shown in Table 5 and only with capacity updating shown in Table 6. The maximum voltage error for the four aging level is less than 2%. Especially for $SoH_5$ aging level is 0.0608 V. The mean and standard deviation absolute value of the terminal voltage error are 0.0205 V and 0.0110 V respectively. What's more, all the SoC estimation errors are less than 0.025. Especially for the battery at $SoH_5$ aging level, the maximum SoC estimation error is 0.024, and the mean error and standard deviation are 0.0122 and 0.104 respectively. Although the SoC estimation performance mainly depends on the accuracy of battery capacity and current sensor, the accuracy of battery model is also important. An erroneous battery model hardly can get reliable SoC estimation. On the other hand, when the model accuracy has been improved, the SoC estimation accuracy will be improved accordingly.

Consequently, we can conclude that both the capacity and ohmic resistance $R_i$ are required to be updated to achieve an optimal performance on battery voltage estimation, SoC estimation and others applications. It is noted that if we can update all the model parameters with pulse currents based on Eqs. (3) and (4), the estimation accuracy will be greatly improved. However, to ensure the control precision of battery system, we can update the $R_i$ parameter and capacity parameter in accordance with our previous experience presented in Refs. [1,6].

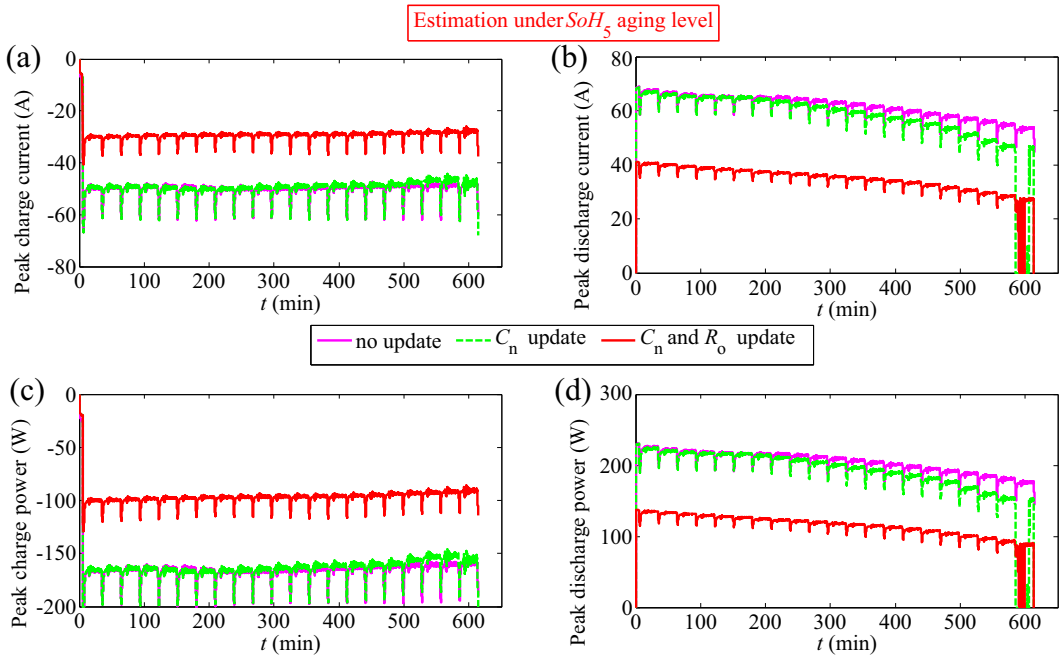


**Fig. 7.** The SoP estimation results for 1 s output: (a) peak charge current; (b) peak discharge current; (c) peak charge power; (d) peak discharge power.

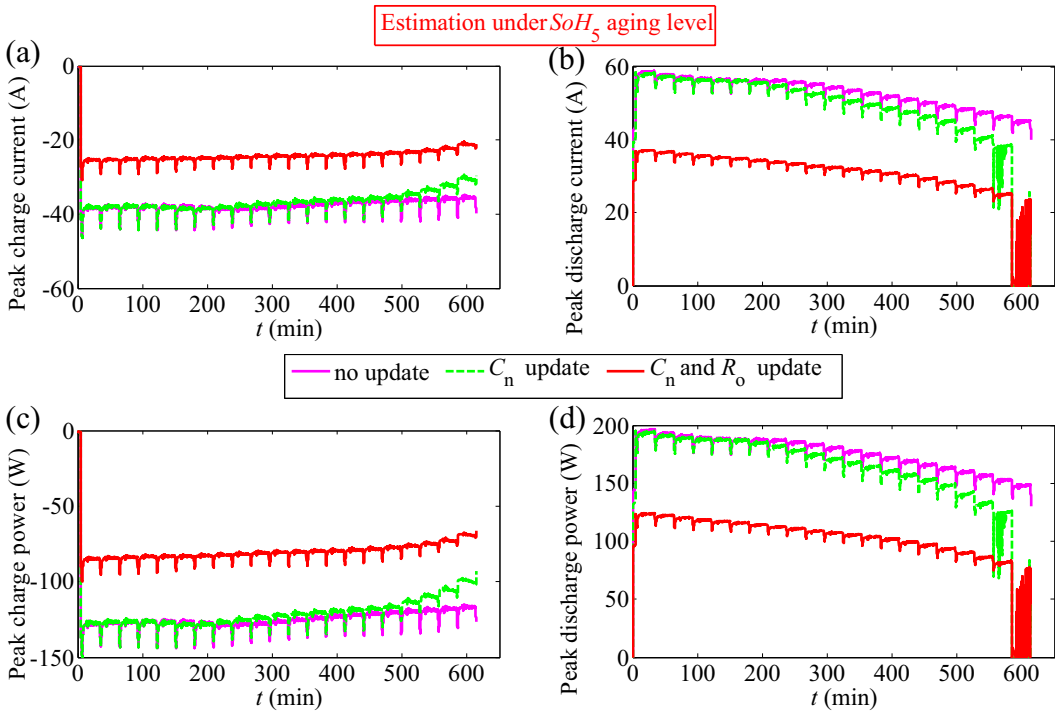


**Fig. 8.** The SoP estimation results for 30 s continuous output: (a) peak charge current; (b) peak discharge current; (c) peak charge power; (d) peak discharge power.

*4.2.3. Joint estimator of battery SoC and SoP*

This section discusses the joint estimator with capacity and $R_i$ parameters updating under the $SoH_5$ aging level. From Table 7, we find that the AEKF-based voltage and SoC estimator with capacity and $R_i$ parameters updating is reliable enough for SoP predicting. Therefore, we can calculate the continuous SoP accordingly. The peak currents and powers for instantaneous and 30 s continuance sampling intervals are shown in Figs. 7 and 8 respectively. It is noted that the initial SoC is incorrectly initialized to 0.5.

From Fig. 7, we find that the peak currents decrease greatly as the battery degrades, therefore the power threshold provide by the battery manufacturer is not reliable. Especially when its health condition is lower than a certain value, the battery will be damaged when using the given threshold. In additional, when the electrified vehicles are operated under the dynamic driving cycles, the threshold of peak power or current should be changed in accordance with the operating condition. From Fig. 7(a), when the actual SoC closes to its higher threshold, the peak charge currents are very small, it can avoid over-charged effectively. On the other hand, the peak discharge currents shown in Fig. 7(b) are very big at this SoC points. But when the actual SoC closes to its lower threshold, the peak discharge currents will be very small. It can avoid over-discharged effectively.

From Figs. 7 and 8, we find that the peak currents will be reduced to 50–60% of level in its fresh state when battery SoH is 0.8. Thus the model used for battery control system is needed to be calibrated periodically.

Therefore, the battery model is less accurate as battery aged. Updating the parameter of battery capacity can improve the estimation accuracy of the SoC estimator noticeably. Updating the parameter of ohmic resistance does not help much in SoC estimation. It is because that the accurate capacity value is the key for SoC calculation. But updating the parameter of ohmic resistance can greatly improve the accuracy of the voltage estimation. Updating all the model parameters achieves even better performance however this may not be easy to achieve in real-time driving. To achieve a desirable prediction precision on battery state, it is a most cost-effective way to update the ohmic resistance and capacity, which has a potential to improve the performance of SoC and SoP joint estimator against battery degradation.

## 5. Conclusions

(1) The lumped parameter battery model is developed to describe the dynamic performance of lithium-ion battery accurately. It is noted that the Nernst model is used to reshape the relationship between battery SoC and the open circuit voltage in this improved model. A discretization method for the battery model has been proposed, and it has the potential to recalibrate the model parameter in real-time.

(2) An adaptive extended Kalman filter has been employed to develop the joint estimator of battery SoC and SoP. The performance of the proposed joint estimator has been discussed and verified by varying aging levels of battery cells. For the UDDS profiles performed of fresh state, the voltage and SoC estimation error are less than 2% and 1% respectively.

(3) A schematic analysis on the need for model parameter update with lowest computation burden has been carried out. The results indicate that the joint estimator with parameter update method can greatly improve the estimation accuracy of battery SoC. What's more, updating the parameter of ohmic resistance and battery capacity can improve the performance of the estimator significantly, and its prediction precision is good enough for electrified vehicles application. The estimation error is less than 2.5% especially for the worst health condition.

## Acknowledgment

This work was supported by the National High Technology Research and Development Program of China (2012AA111603, 2013BAG05B00, 2011AA11A290) in part, the National Natural

Science Foundation of China (51276022) and the Higher School Discipline Innovation Intelligence Plan ("111"plan) in part, and the Program for New Century Excellent Talents in University (NCET-11-0785) in part.

## References

[1] R. Xiong, F. Sun, Z. Chen, H. He, Appl. Energy 113 (2014) 463–476.
[2] R. Xiong, F. Sun, X. Gong, H. He, J. Power Sources 242 (2013) 699–713.
[3] R. Xiong, X. Gong, C.C. Mi, F. Sun, J. Power Sources 243 (2013) 805–816.
[4] G.L. Plett, J. Power Sources 161 (2006) 1369–1384.
[5] R. Xiong, H. He, F. Sun, K. Zhao, IEEE Trans. Veh. Tech. 62 (2013) 108–117.
[6] R. Xiong, H. He, F. Sun, K. Zhao, Energies 5 (2012) 1455–1469.
[7] F.C. Sun, R. Xiong, H. He, W.Q. Li, J.E.E. Aussems, Appl. Energy 96 (2012) 3773–3785.
[8] G.L. Plett, IEEE Trans. Veh. Tech. 53 (2004) 1586–1593.
[9] R. Klein, N.A. Chaturvedi, J. Christensen, J. Ahmed, R. Findeisen, A. Kojic, IEEE Transac. Contr. Syst. Technol. 21 (2013) 289–301.
[10] Andreas Rauh, Saif S. Butt, Harald Aschemann, Int. J. Appl. Math. Comput. Sci. 23 (2013) 539–556.
[11] A. Baba, S. Adachi, in: 2012 IEEE International Conference on Control Applications (CCA), 2012, pp. 409–414.
[12] M. Gholizadeh, F.R. Salmasi, IEEE Trans. Ind. Electron. 61 (2014) 1335–1344.
[13] J. Li, J.K. Barillas, C. Guenther, M.A. Danzer, J. Power Sources 230 (2013) 244–250.
[14] M. Mastali, J. Vazquez-Arenas, R. Fraser, M. Fowler, S. Afshar, M. Stevens, J. Power Sources 239 (2013) 294–307.
[15] G.L. Plett, J. Power Sources 134 (2004) 252–261.
[16] G.L. Plett, J. Power Sources 134 (2004) 262–276.
[17] G.L. Plett, J. Power Sources 134 (2004) 277–292.
[18] A. Szumanowski, Y. Chang, IEEE Trans. Veh. Technol. 57 (2008) 1425–1432.
[19] R. Xiong, H. He, F. Sun, X. Liu, Z. Liu, J. Power Sources 229 (2013) 159–169.
[20] Wladislaw Waag, Christian Fleischer, Dirk Uwe Sauer, J. Power Sources 242 (2013) 548–559.
[21] R. Xiong, F. Sun, H. He, T. Nguyen, Energy 63 (2013) 295–308.
[22] B. Pattipati, C. Sankavaram, K.R. Pattipati, IEEE Transac. Syst. Man Cybern. C 41 (2011) 869–884.
[23] H. He, R. Xiong, J. Fan, Energies 4 (2011) 582–598.
[24] C. Zhang, J. Jiang, W. Zhang, S.M. Sharkh, Energies 5 (2012) 1098–1115.
[25] Simon Schwunk, Sebastian Straub, Max Jung, J. Electrochem. Soc. 160 (2013) A2155–A2159.
[26] H. Rahimi-Eichi, F. Baronti, M.-Y. Chow, in: 2012 IEEE International Symposium on Industrial Electronics (ISIE), 2012, pp. 1336–1341.
[27] X. Hu, S. Li, H. Peng, F. Sun, J. Power Sources 217 (2012) 209–219.
[28] E.A. Wan, A.T. Nelson, Kalman Filtering and Neural Networks, John Wiley & Sons, 2001, pp. 123–173 (Chapter 5).